



Universiteit
Leiden
The Netherlands

Anisotropy, multivalency and flexibility-induced effects in colloidal systems

Verweij, R.W.

Citation

Verweij, R. W. (2021, May 27). *Anisotropy, multivalency and flexibility-induced effects in colloidal systems*. *Casimir PhD Series*. Retrieved from <https://hdl.handle.net/1887/3179461>

Version: Publisher's Version

License: [Licence agreement concerning inclusion of doctoral thesis in the Institutional Repository of the University of Leiden](#)

Downloaded from: <https://hdl.handle.net/1887/3179461>

Note: To cite this publication please use the final published version (if applicable).

Cover Page



Universiteit Leiden



The handle <https://hdl.handle.net/1887/3179461> holds various files of this Leiden University dissertation.

Author: Verweij, R.W.

Title: Anisotropy, multivalency and flexibility-induced effects in colloidal systems

Issue Date: 2021-05-27

1 Introduction



WHAT do clouds, whipped cream, milk, photographic film, cheese, smoke and marshmallows have in common with each other? One possible answer to that question is that these are all examples of colloidal dispersions. In general, a colloidal dispersion is a phase-separated mixture in which the dispersed phase has a typical size of approximately one nanometer up to a few micron. In addition to their abundance in everyday life, colloids are extensively studied in materials science,¹⁻⁴ the food industry,⁵ for pharmaceutical purposes⁶⁻⁹ and for their fundamental properties,¹⁰⁻¹⁶ among other applications. In this work, we focus on one class of colloidal dispersions, in which the dispersed phase consist of mostly solid particles that are micron-sized, which from now on we call colloids or colloidal particles.

The typical size of colloidal particles sets them apart for two reasons: first, it is large enough for colloids to be observed using conventional light microscopy techniques. This is in stark contrast to, for example, molecular systems, which have length scales below a nanometer, or biological proteins, which can be tens of nanometers in size. Direct experimental measurements of dynamic properties in (bio)molecular systems are challenging because they require single-molecule measurement techniques with high spatial and temporal resolution. Instead, colloidal particles have been widely used as model systems for (macro)molecular structures,¹⁷⁻¹⁹ because their behavior can be captured by simpler experimental techniques. Secondly, their size is small enough so that they are sensitive to thermal fluctuations, which makes them suitable as model systems for their smaller counterparts.

The properties of colloids that we will investigate here can be roughly divided into two topics: first, interactions between the colloidal particles and their environment. These include electrostatic interactions between a particle and a substrate or the hydrodynamic properties of different types of colloidal particles. Second, we study inter-particle interactions, such as the self-assembly of colloidal particles into larger structures. For both topics, it is important to know some fundamental properties of colloid science, which we will now briefly introduce.

Colloidal interactions

There is a large variety of interactions that can take place between colloidal particles and between colloids and their environment. Examples include electrostatic,^{20,21} Van der Waals,^{20,22} depletion,^{23,24} magnetic,^{25,26} hydrophobic/hydrophilic,^{27,28} critical Casimir^{29,30} or hydrodynamic interactions,³¹⁻³⁷ and many more. We will discuss some of the interactions that are relevant to the current work in this section.

Generally speaking, these interactions can be classified as either attractive or re-

pulsive and as either specific or nonspecific. For use in practical applications, it is of vital importance that the colloids are stable,³⁸ which means that the particles remain dispersed in the medium and do not form undesired aggregates. To this end, nonspecific attractive interactions need to be balanced by repulsive interactions.

Nonspecific attractive forces that tend to destabilize colloids are typically Van der Waals, or dispersion forces, which are attractive forces that arise from the interactions between instantaneous multipoles of the atoms and molecules that constitute the particles.^{20,22} These interactions strongly depend on the distance r between colloids and decay as $1/r^6$.

Another example of nonspecific attractive forces are electrostatic interactions between surfaces of opposite charge, when attraction between the two surfaces is undesired, as is often the case between colloidal particles and the container walls, for example. In ionic solutions, electrical double layers are formed around charged surfaces, which consist roughly of a layer of adsorbed ions at the colloid surface and a diffuse layer of counterions further away from the surface.^{20,39} Interactions between double layers of surfaces that carry opposite charges lead to an attractive force between them. Naturally, electrostatic interactions can also be used to encode (desired) specific repulsive interactions between colloids. In that case, the colloids are functionalized in such a way that their surface charge is nonzero and of the same sign. Like-charge repulsion between their electrical double layers then leads to colloidal stability, if this repulsion is greater than the nonspecific attractive forces acting on the particles.

A second important example of repulsive interactions between colloidal particles are entropic repulsive forces.⁴⁰ To that end, polymer chains are grafted on the surface of colloidal particles at a sufficient area density.^{41,42} When two polymer coated particles approach each other, the polymer layers start to overlap. Because of excluded volume interactions between the polymer strands, the configurational entropy of the polymers is reduced: they have less room to move. This loss of configurational entropy results in an effective entropic repulsive force between the particles.⁴² This method of entropic stabilization is also known as steric stabilization.

On the other hand, it is often desirable to form aggregates of colloidal particles that have specific properties, such as the desired size or shape. To enable the formation of specific clusters of colloidal particles, attractive interactions have to be used that act only between specific sets of particles. Examples include the electrostatic attraction of oppositely charged surfaces that was already discussed, depletion interactions,^{23,24} magnetic interactions,^{25,26} critical Casimir interactions,^{29,30} or hydrophobic interactions.^{27,28} Specifically, hydrophobic interactions are of interested in the context of this work, as these are responsible for the formation of the lipid bilayers^{43–46} that form an integral part of the colloidal model systems presented here. Hydrophobic interactions cause dispersed objects that are nonpolar to maximize their contact with other hydrophobic surfaces, in order to minimize their contact with the surrounding aqueous medium. The exact origin of these interactions is not fully understood, but most likely originates from entropic effects, caused by the disruption of hydrogen

bond formation between water molecules by the hydrophobic moieties.⁴⁷

Self-assembly

Having discussed some examples of possible attractive and repulsive interactions between colloidal particles, we are interested in studying how the interactions between colloidal building blocks can be used for bottom-up assembly of larger structures and materials. Such a bottom-up assembly process, where interactions between colloidal particles lead to the formation of specific structures without additional external input, is known as colloidal self-assembly.^{3,4,28,48–58} Colloidal self-assembly has been used to fabricate a large variety of different structures that can have specific desired properties, such as specific crystal lattices that have photonic band gaps^{1,2,59,60} or biomimetic materials that can be used as model systems for biological systems.^{61–65}

Self-assembly requires specific interactions that can be provided by specialized molecules that can act as linkers between the colloids. For example, by using synthetically produced deoxyribonucleic acid (DNA) strands, DNA linkers can be fabricated. To understand how this works, we now briefly discuss the structure of the DNA double helix. The double helix structure of DNA is depicted schematically in Figure 1.1a. It consists of two sugar phosphate backbones that support a sequence of nucleobases. There are four nucleobases which each bind specifically only to one of the other bases, forming a base pair via hydrogen bonding: adenine (A) binds to thymine (T) and cytosine (C) binds to guanine (G). The complementary strands run in opposite directions, so that the 5'-end of one strand aligns with the 3'-end of the other. Figure 1.1b shows an electron microscopy image of a bundle of DNA strands, where the pitch of the DNA double helix structure is clearly visible.

By synthesizing two DNA strands that are complementary except for a few base pairs at the end, a double-stranded DNA linker is formed after hybridization, that contains a single-stranded overhang, or sticky end. As depicted in Figure 1.1c, by using two of these DNA linkers with complementary sticky ends, the linkers specifically bind with each other via Watson-Crick base pairing. Because of the high specificity of DNA hybridization, these DNA strands can act as an “intelligent glue” between the micron-sized colloidal particles. As shown in Figure 1.1d, DNA linkers can for instance be employed to induce the crystallization of colloidal particles, which can be controlled by changing the temperature around the melting temperature of the sticky end.⁶⁹ DNA linkers have been employed in a large number of self-assembly studies^{4,69–76} where a great variety of colloidal objects and materials with great potential for interesting applications were fabricated.

Apart from inter-particle interactions, there are two other important kinetic effects that are instrumental in self-assembly processes. First, in general, a colloidal system used for self-assembly starts in a state that is not in thermal equilibrium. Then, the free energy of the system is reduced during self-assembly, until either a local or a global minimum in the free energy of the system is reached. This can cause problems if the system can not transition from a certain local minimum in the free energy

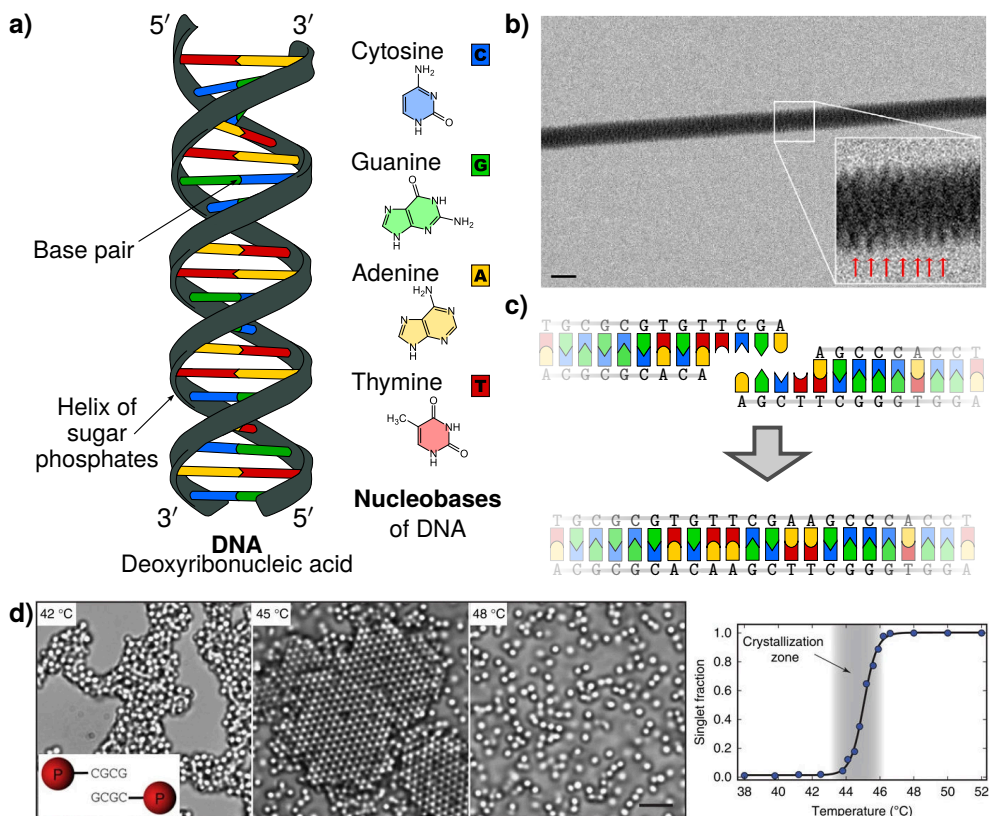


Figure 1.1: Structure of DNA and crystallization of DNA coated colloids. **a)** Schematic depiction of the DNA double helix and its base pairs: cytosine (C), guanine (G), adenine (A) and thymine (T). The two complementary strands run in opposite directions, so that the 5'-end of one strands aligns with the 3'-end of the other. **b)** Electron microscopy (EM) image of λ -DNA fibers. The inset zooms in on a part of the fiber, the red arrows indicate the 2.7 nm pitch of the double helix. Scale bar is 20 nm. **c)** Example of the hybridization of two complementary DNA sticky ends, consisting of four base pairs. The sequence is taken from the human hemoglobin α -subunit gene. **d)** Brightfield images showing the morphologies of amorphous (left, 42 °C), crystalline (middle, 45 °C) and unbound (right, 48 °C) assemblies of DNA-coated 1 μ m colloids. Scale bar is 5 μ m. Inset: schematic illustration of DNA-coated particles. The DNA is grafted to the particle surfaces. The particles are functionalized with DNA linkers that have CGCG (palindrome) sticky ends. Right: singlet particle fraction (unbound particles) of DNA-coated colloids as a function of temperature. The temperature window over which particle crystallization occurs is shaded. *Attribution: a) Reprinted (adapted) with permission from Gentile et al.⁶⁶ Copyright 2012 American Chemical Society. b) Adapted from "Difference DNA RNA" by Sponk⁶⁷ (CC BY-SA 3.0), via Wikimedia Commons. c) Adapted from "Ligation" by Ball⁶⁸ (CCO 1.0), via Wikimedia Commons. d) Adapted from Wang et al.⁶⁹ (CC BY 4.0).*

to the desired global minimal free energy state. In that case, the system is said to be kinetically arrested.⁷⁷ Various solutions have been proposed to overcome these kind of equilibration issues, such as by thermally annealing the system,^{78,79} using directional interactions for greater control over the self-assembly pathway^{51,53,80–83} or by using structures that are reconfigurable after they have formed.^{57,58,84,85}

The second kinetic factor that determines the success of self-assembly is related to the typical range of the attractive interactions. By its definition, in colloidal self-assembly, interactions are local and therefore, typically short-ranged. This means that the rate at which particles approach each other close enough for them to interact has a large effect on the rate of the self-assembly process.^{86,87} In the absence of external forces, mixing is typically a purely passive process, driven by the random diffusion or Brownian motion of the particles. Therefore, the diffusive properties of the constituents and their hydrodynamic interactions are of key importance to self-assembly processes as well.³⁶

Brownian motion

The Brownian motion of colloidal particles is a central focus of this work. Brownian motion, which was first observed by the botanist Robert Brown in 1827, is well described by the (translated) words of Jean-Baptiste Perrin:¹⁹ *“...all the particles situated in the liquid, instead of assuming a regular movement of fall or ascent, according to their density, are, on the contrary, animated with a perfectly irregular movement. They go and come, stop, start again, mount, descend, remount again, without in the least tending toward immobility.”* We can make sense of this chaotic process by considering the first and second order moments of the particle displacements $\Delta\mathbf{r}(t + \tau)$ between a time t and a time $t + \tau$ later, where τ is the lag time between displacements. The first moment, $\langle \Delta\mathbf{r}(t + \tau) \rangle$ is equal to zero, which states that the average position of particles experiencing Brownian motion does not change in time. The amount of motion of the particles can instead be characterized by the second moment of particle displacements, or the mean squared displacement (MSD), which is equal to

$$\langle (\Delta\mathbf{r}(t + \tau))^2 \rangle = 2dD\tau, \quad (1.1)$$

with d the number of dimensions. D is the diffusion coefficient which characterizes the mobility of the particles. Einstein¹⁷ and others^{18,92} showed how this diffusion coefficient is related to the thermodynamic properties of the fluid and the size of the particle. For a spherical particle, the diffusion coefficient can be calculated using the Stokes-Einstein relation:^{17,93}

$$D_{\text{sph.}} = \frac{k_B T}{6\pi\eta R_{\text{sph.}}}, \quad (1.2)$$

where k_B is the Boltzmann constant, used to describe the average thermal energy of each degree of freedom in a thermodynamic system, which equals $\frac{1}{2}k_B T$. The absolute temperature of the system is given by T , η is the viscosity of the medium and $R_{\text{sph.}}$ is the radius of the sphere.

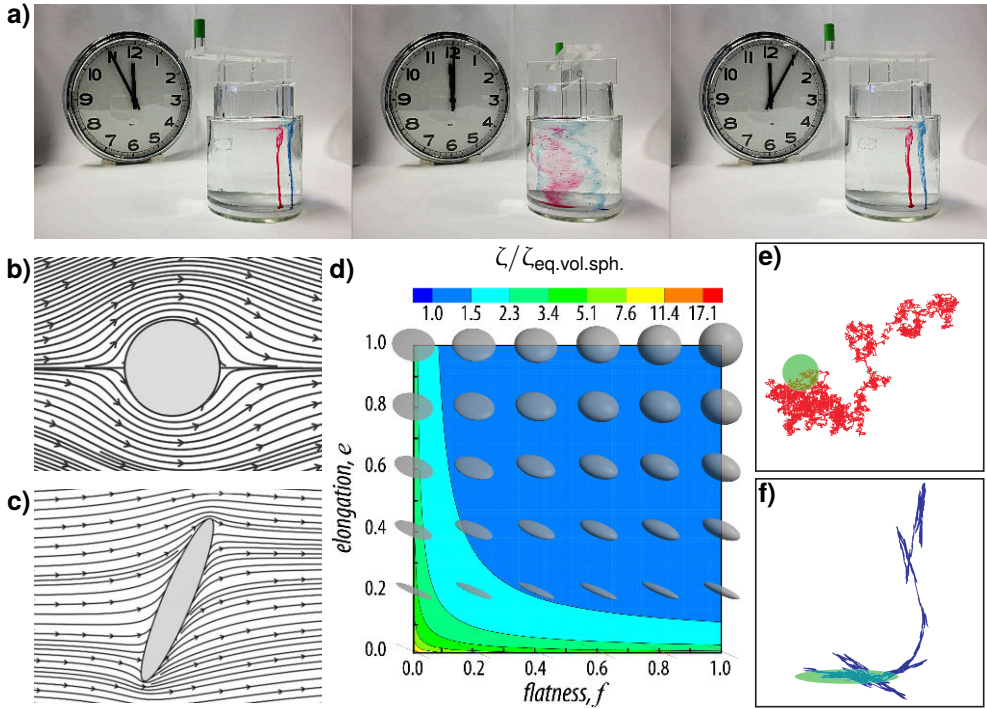


Figure 1.2: Low Reynolds number hydrodynamics. **a)** Left: Dye is injected in a viscous fluid (low Re) between two cylinders. Center: Rotating the fluid in one direction mixes the dyes and the fluid. Right: After the same amount of turns in the opposite direction, the dyes return to their approximate initial position. **b)** Streamlines of the 3D flow field around a 6:1 prolate spheroid in the equatorial plane, obtained by integration of the full Navier-Stokes equations at $Re = 1$ for an attack angle of 90 deg (the angle between the flow direction and the long axis). **c)** Streamlines for the same spheroid as in panel b, but now in the meridional plane for an attack angle of 67.5 deg. **d)** The ratio between the drag coefficient ζ of ellipsoids and the drag coefficient $\zeta_{\text{eq.vol.sph.}}$ of a sphere of the same volume as the ellipsoid shows marked size effects as function of flatness and elongation. **e)** Simulation of a 2D random walk for a sphere with diffusion coefficients $D_a = D_b = 0.5$. **f)** Same as in panel e, but for an ellipsoid with $D_a = 0.99$, $D_b = 0.01$. The total diffusion coefficient $D = (D_a + D_b) = 1.0$ is the same for both particles in panels e and f. Trajectories are shown during the time it takes an ellipsoid to rotate 1 rad. During this time, the behavior of the sphere (self-similar isotropic random walk) is very different from the ellipsoid (quasi 1D diffusion along the long axis). At longer times, the coarse-grained trajectories of both shapes correspond to an isotropic random walk. Attribution: a) Adapted from "Time reversible flow demonstration" by Ved1123⁸⁸ (CC BY-SA 4.0), via Wikimedia Commons. b+c) Reprinted by permission from Springer Nature: Andersson and Jiang,⁸⁹ copyright Springer Nature 2019. d) Reprinted from Bagheri and Bonadonna,⁹⁰ with permission from Elsevier. e+f) From Han et al.⁹¹ Reprinted with permission from AAAS.

Because of their small size, colloidal particles behave very differently in fluids compared to larger objects. A striking example is shown in Figure 1.2a, where two dyes are injected into a viscous fluid that is sandwiched between two cylinders. By rotating the cylinders with respect to each other, the fluid is sheared and the dyes and fluid mix, as shown in the center panel of Figure 1.2a. Amazingly, by rotating the cylinders by the same amount but in the opposite direction, the dyes return to their original position, as shown in the last panel of Figure 1.2a. The dyes are only slightly more spread out compared to their original position, which is caused by diffusion of the dye molecules in the intermediate time. Apart from this, the behavior of the dye particles in the viscous fluid shows time-reversal symmetry.

This behavior, which is not limited to “viscous” fluids, can be characterized by the Reynolds number Re , which is defined as³¹

$$Re = \frac{\rho_p u L_p}{\eta}, \quad (1.3)$$

with ρ_p the mass density of the particle, u the velocity of the particle with respect to the fluid, L_p the typical dimension of the particle (e.g. the radius in case the particle is spherical) and η the viscosity of the fluid. Reynolds numbers can be roughly characterized as high ($Re \gtrsim 10^3$) or low ($Re \lesssim 10$). A high Reynolds number is what we are typically used to in everyday life: for a human swimming in water*, $Re \approx 10^6$. In the high Reynolds number regime, flows are turbulent and the motion no longer has time-reversal symmetry: that means that if the swimmer moves their arms and legs in a symmetric back-and-forth motion, they can propel themselves. Conversely, at low Reynolds numbers, there is time-reversal symmetry. That means that a human swimming in peanut butter* ($Re \approx 4$) has to perform asymmetric forward and backward strokes, or they will be stuck in the same position indefinitely. The same holds true for colloidal particles: for micron-sized silica particles in water, the Reynolds number $Re \ll 1$. Fluid flows around the particle are therefore not turbulent, but laminar, as shown in Figure 1.2b for a circular cross section of a colloidal particle.

In addition to spherical particles, the Brownian motion at low Reynolds number of colloids of various shapes have been studied. These include ellipsoids,^{91,95,96} boomerangs^{14,97,98} and clusters.^{12,13} These studies have revealed that shape affects the diffusive motion at short timescales. For example, it can be seen that the flow field around a circular cross section of an ellipsoid (Figure 1.2b) is very different from the flow field around a different cross section in the meridional plane,⁸⁹ as shown in Figure 1.2c. Moreover, as shown in Figure 1.2d, the drag coefficient ζ is also greatly affected by the shape of the particle. For a drag coefficient $\zeta = k_B T / D_T$, with D_T the translational diffusion coefficient, it was found that anisotropic particles typically have a higher drag coefficient compared to spheres of the same volume.⁹⁰

*Here, $\rho_p = 1000 \text{ kgm}^{-3}$, $u = 1 \text{ ms}^{-1}$, $L_p = 1 \text{ m}$ and $\eta = 0.001 \text{ Pa s}$ for water and $\eta = 250 \text{ Pa s}$ for peanut butter.⁹⁴ It is possible that the swimming speed will be lower in peanut butter, which will lower the Reynolds number further.

The drag coefficient of anisotropic particles is typically different along different particle symmetry axes. By comparing a random walk of a spherical particle in Figure 1.2e to that of an ellipsoidal particle in Figure 1.2f, it becomes apparent that they show very different trajectories.⁹¹ While the sphere performs a self-similar isotropic random walk, the ellipsoid performs a quasi one-dimensional random walk in the direction of its long axis. Therefore, for particles of anisotropic shape at short timescales, Equation 1.1 can be generalized as follows

$$\langle X_i(t + \tau) X_j(t + \tau) \rangle = 2D_{ij}\tau, \quad (1.4)$$

where $X_i(t + \tau)$ is a generalized displacement corresponding to one of the degrees of freedom labeled by i (i.e. translational, rotational, ...) and D_{ij} is the element of a generalized diffusion tensor which relates the mobility of particle displacements corresponding to the degrees of freedom i and j . Diagonal elements of D where $i = j$ describe properties such as the translational diffusivity and the rotational diffusivity. Additionally, different diffusive modes can be coupled, e.g. helical particles rotate as they translate and vice versa.⁹⁹ These modes are described by the off-diagonal elements where $i \neq j$.

In general, the diffusion tensor D depends on the shape and size of the particle studied. Similarly to what is known for spherical particles, displacements of anisotropic particles are typically larger in directions that correspond to smaller hydrodynamic drag.^{12-14,16,91,97} Therefore, the ellipsoid in Figure 1.2f primarily diffuses along its long axis at shorter timescales than the rotational diffusion time. The rotational diffusion time characterizes the time it takes for the particle to rotate 1 rad. At longer timescales, the influence of particle shape decreases, as the shape effects are averaged out because of rotational diffusion.⁹¹

While the Brownian motion of rigid particles has been extensively studied, little is known about the diffusive properties of flexible particles, that change their shape as they diffuse. This question is highly relevant, because many (macro)molecular systems found in nature display segmental flexibility. For most of these, reconfigurability also affect the biological function of the compound.¹⁰⁰⁻¹⁰⁴ For such flexible structures, the diffusion tensor D_{ij} contains terms related to these internal deformation modes.¹⁰⁵⁻¹⁰⁸ In turn, this shows that couplings between deformation modes and other degrees of freedom, such as translational or rotational diffusivity, are possible. The study of the diffusive properties of flexible structures is the main subject of Chapters 5-7.

Colloid-supported lipid bilayers

The study of the diffusivity of flexible colloidal structures was made possible by the development of DNA linker-functionalized colloid-supported lipid bilayers¹¹⁰⁻¹¹² (CSLBs). CSLBs are used in a diverse range of research areas and applications,¹¹³ which range from drug delivery,^{7-9,114-117} to bio-sensing applications^{15,118} and more fundamental studies on lipid phase separation.^{64,65} Of special interest to this work

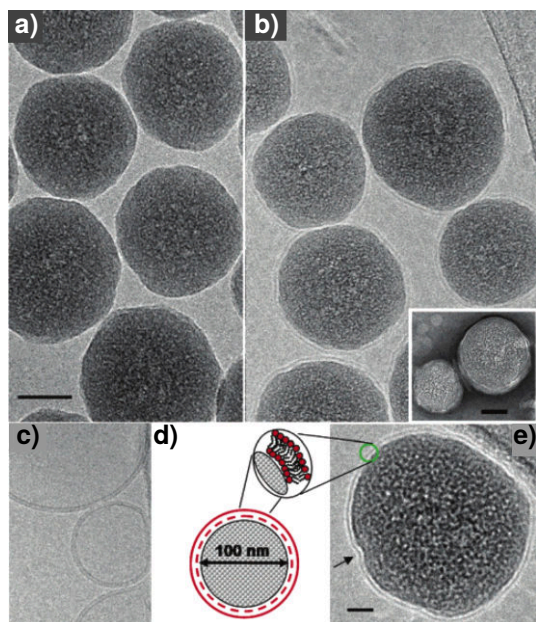


Figure 1.3: Cryo-EM images of colloid-supported lipid bilayers (CSLBs). **a)** 110 nm silica nanoparticles. The scale bar is 50 nm, the same magnification is used in panels b and c. **b)** Bilayer-functionalized silica nanoparticles formed by the rupture and spreading of liposomes. Inset: CSLBs imaged using a negative staining method. Scale bar is 50 nm. **c)** Several liposomes, the polar head groups of the two lipid layers are visible (darker rings). **d)** Schematic of a nanoparticle surrounded by a lipid bilayer. **e)** The bilayer is in close contact with the particle surface. Scale bar is 20 nm. Attribution: Reprinted (adapted) with permission from Mornet et al.¹⁰⁹ Copyright 2004 American Chemical Society.

are self-assembly applications.^{85,110–112} Various properties of CSLBs are discussed extensively in Chapters 3–7.

CSLBs consist of solid colloidal particles surrounded by a fluid lipid bilayer. In Figure 1.3a, cryo-EM images of colloidal nanoparticles are shown, which can be functionalized with a lipid bilayer, as can be seen from Figure 1.3b. The bilayer is formed by the adhesion and rupture of small liposomes (shown in Figure 1.3c) on the particle surface. As depicted graphically in Figure 1.3d and shown in the cryo-EM image in Figure 1.3e, the bilayer is in close contact with the particle surface and follows its overall shape. Therefore, the particles act as a scaffold for the lipid bilayer. The shape of the particle in turn sets the shape of the lipid bilayer.⁸⁵ Interestingly, DNA linkers that are functionalized with a hydrophobic end group, or anchor, can be inserted into the bilayer surrounding the particle, via hydrophobic interactions between the lipids and anchor. Because of the fluidity of the bilayer, these linkers can freely surf over the particle.^{110–112} Then, by functionalizing two sets of particles with two different DNA linkers with complementary sticky ends, self-assembled clusters of CSLBs can be formed that are bonded by the DNA linkers. But because the DNA linkers can diffuse over the particle surface, the particles in the cluster can also move with respect to one another, while remaining permanently bonded.

CSLBs surrounded by fluid membranes with surface-mobile binding groups are of great interest to a wide range of applications and fundamental problems. The flexible bonds that are provided by CSLBs open the door to answering numerous fundamental questions where flexibility plays a role, such as the study of the relation

between internal deformation modes and Brownian motion. In addition, their reconfigurability should allow for easier relaxation of self-assembled structures towards thermal equilibrium. This will enable the study of structural flexibility and its impact on phase behavior, such as in lattices that have a specific crystal structure or other sought after properties.^{57,58,119,120} Furthermore, CSLBs, because of their lipid bilayer, can be thought of as biomimetic particles and are therefore of interest to model membrane and cell biology studies,^{61–65} smart drug delivery^{7–9,114–117} and bio-sensing applications.^{15,118} Lastly, they may be used as building blocks in the fabrication of nano- to micron-sized robotic devices.^{121–125}

Outline of this thesis

In this thesis, we study the impact of particle shape anisotropy, multivalent interactions and flexibility on systems of colloidal particles. This thesis is structured as follows:

In **Chapter 2**, we study the behavior of colloidal dimer particles that diffuse above a planar wall. Our results highlight the rich dynamics that nonspherical particles exhibit in the proximity of walls and can aid in developing quantitative frameworks for the dynamics of arbitrarily-shaped particles in confinement.

Having studied rigid anisotropic particles in Chapter 2, in the next chapters we extend this to anisotropic particles that have internal deformation modes. In Chapters 3–4, we study the fundamental properties of DNA-functionalized CSLBs, which form the basic building blocks of anisotropic colloids with flexible bonds. This, in turn, enables the study of flexibility on their conformational and diffusive properties in Chapters 5–7.

Specifically, in **Chapter 3**, we have studied colloidal systems that have internal degrees of freedom that allow for shape changes: CSLBs. We show how to optimize their functionalization, in order to obtain particles suitable for self-assembly experiments, which requires well-stabilized colloids with a homogeneous bilayer that is fully fluid.

Then, in **Chapter 4**, we have studied the multivalent interactions between DNA linker-functionalized CSLBs that can form flexible bonds. We characterize how linker depletion effects^{84,126} could be used to limit the valency of self-assembled clusters made of CSLBs.

By taking advantage of the ability to limit the valency of clusters of CSLBs using low DNA linker concentrations, in **Chapter 5**, we have formed flexibly-linked colloidal chains of three CSLBs. We have measured the full diffusion tensor of these flexible trimers and have found marked flexibility-induced effects.

Based on these results, in **Chapter 6**, we study the conformational and diffusive behavior of flexibly-linked colloidal chains of three to six CSLBs. There, we find that the behavior of these chains can be described using results from polymer theory.

Because of their unique topology, in **Chapter 7**, we have assembled flexible rings of four and six CSLBs. We have quantified the differences between flexible chains, loops and domino lattices. Our findings could have implications for the flexibility of

floppy colloidal materials.

Finally, in the last chapter, we provide a short outlook on how to synthesize flexibly-linked particles with directional interactions. Our work demonstrates the rich dynamics and possibilities for applications of reconfigurable colloidal systems.